**Boise State University**
## ScholarWorks

Materials Science and Engineering Faculty
Publications and Presentations

Department of Materials Science and Engineering

# Effect of Grain Boundary Engineering on Microstructural Stability During Annealing

Scott M. Schlegel
*Boise State University*

Sharla Hopkins
*Boise State University*

Megan Frary
*Boise State University*

# Effect of Grain Boundary Engineering on Microstructural Stability during Annealing

Scott M. Schlegel, Sharla Hopkins, and Megan Frary

Department of Materials Science and Engineering, Boise State University

## ABSTRACT

Grain boundary engineering, which increases the special boundary fraction, may improve microstructural stability during annealing. Different processing routes are undertaken to establish the effectiveness of each and to better understand which microstructural features determine the resulting stability. We find that multiple cycles of grain boundary engineering result in a material that resists abnormal grain growth better than other processing routes despite similarities in special boundary fraction, grain size, and general boundary connectivity among as-processed materials.

**Keywords**: grain boundary engineering, abnormal grain growth, grain boundary connectivity, copper, texture

## INTRODUCTION

Many materials properties depend on grain boundary character [1-7]. For example, some coincidence site lattice (CSL) boundaries, characterized by a $\Sigma$ value which gives the reciprocal density of coincident sites, have been shown to be resistant to intergranular cracking [1-3] and corrosion [4-6]. As a result of their "special" properties, a high fraction of low-$\Sigma$ CSL boundaries is desirable in a microstructure. Watanabe introduced the concept of grain boundary engineering (GBE) in which a high fraction of special boundaries ($\Sigma \leq 29$) is imparted to a material [8]. While boundaries with $\Sigma \leq 29$ are usually classified as special, not all of these demonstrate so-called "special behavior," which is most often found in $\Sigma 3^n$ boundaries. Through GBE processing, the fraction of special boundaries, $p$, typically between 0.3 to 0.6 in conventionally processed materials, can be increased to $p \sim 0.8$ [1-7]. The improved properties resulting from the increase in the special fraction are likely due in part to the corresponding decrease in the connectivity of general grain boundaries [9, 10].

Grain boundary engineering can also affect microstructural stability during annealing. Schwartz *et al.* investigated the influence of processing method and annealing temperature on the grain boundary character distribution (GBCD) in high-purity copper [11]. The grain size and GBCD of the specimen processed by GBE were stable during annealing, while a conventionally processed specimen experienced abnormal grain growth (AGG) and a slight decrease in $p$ [11]. Grain boundary character has also shown to influence microstructural stability in Ni-based alloys [7, 12]. Tan *et al.* found the GBCD remained much more stable in GBE'd materials as compared to as-received materials after annealing for 6 weeks [12].

A number of other studies have investigated how the GBCD evolves during grain growth, regardless of the initial distribution of boundary types [13, 14]. In general, high-energy boundaries are expected to exhibit higher mobilities than low-energy boundaries (e.g., some low-$\Sigma$ CSL boundaries). Lee and Richards found grain growth in nickel to increase the special boundary fraction which they attributed to the relative boundary mobilities [13]. Lower-energy, lower-mobility boundaries should increase in length as higher-mobility boundaries would likely be consumed during grain growth. However, another study of nickel with an initially high special fraction resulted in

decreased $p$ after grain growth [14], perhaps an effect of minimized solute-boundary interactions, which inhibit mobility via Zener pinning, in low-energy boundaries. Therefore, annealing may increase $p$ in high purity metals, while $p$ is expected to decrease with grain growth in samples with impurities.

The objectives of the present investigation are to further study the microstructural stability of grain boundary engineered versus conventionally processed copper, to investigate conditions that lead to the onset of abnormal grain growth in these materials, and to determine the role that general boundary connectivity plays in microstructural stability.

## EXPERIMENTAL PROCEDURE

The material used in annealing experiments was 99.9% Cu bars. Two processing routes were applied: (1) cyclic GBE or (2) one-step "conventional processing" (CP). One cycle of GBE consists of cold rolling to 80% of the original thickness followed by annealing in air for 10 min at 560°C then water quenching; GBE parameters were adapted from [11]. The GBE process was repeated four times, and after each cycle, 20% of the specimen length was removed for microstructural characterization; these specimens are referred to as 0GBE, 1GBE, 2GBE, 3GBE, and 4GBE. The CP route used a single strain step to reduce the thickness by the same amount accumulated during four GBE cycles (59%), followed by the same annealing step as in GBE processing.

Processed Cu specimens were annealed in air at 700°C for 2, 12, 36, and 108 h, at 800°C for 6 and 18 h, and at 900°C for 8 h. After annealing, standard metallographic sample preparation was used followed by electropolishing for 20 min at 1.8 V in a solution of 70% phosphoric acid at room temperature. Grain orientation and grain boundary character were determined using an EDAX/TSL electron backscatter diffraction (EBSD) system on a LEO 1430 SEM. Orientation data were collected on a hexagonal grid with a step size of 2 µm over a 1 mm$^2$ area and analyzed with OIM™ Analysis software. The scan data were cleaned using the neighbor-orientation correlation algorithm. Microstructural evolution was quantified by determining mean linear intercept grain size, special boundary length fraction and crystallographic texture. Customized data analysis routines in IDL (RSI, Inc., Boulder, CO) were used to determine the general boundary connectivity via the cluster mass distribution [10]. A connected path of general boundaries, which can span many grains, is defined as a boundary cluster; the extent of the cluster is described by its mass, the total length of boundaries in the cluster normalized by the mean linear intercept, $\overline{L}$ . Here, areas $35 \times 35\ \overline{L}^2$ were analyzed for each sample resulting in an analysis of approximately 1225 grains. By analyzing areas with more than 1000 grains, errors are limited to only the largest cluster sizes which can be viewed as a lower bound on the true size of general boundary clusters. A thorough discussion of the error inherent in this analysis is provided in [10].

## RESULTS AND DISCUSSION

The goal of GBE processing was to increase the special boundary fraction ($\Sigma \leq 29$) in copper. After four cycles of GBE, $p$ increased from 0.35 to 0.64; Figure 1 shows the GBCD for each processing condition where the majority of special boundaries are seen to be $\Sigma 3$ boundaries. Among CSL boundaries, the populations of $\Sigma 9$ and $\Sigma 27$ are also significant; of the other CSL boundaries with $\Sigma \leq 29$ (~0.06), none had a population greater than 0.015. The fraction of low-angle boundaries was initially high in the as-received material (0GBE) and decreased to a relatively constant value of about 2% after processing. In addition to changing the special fraction, GBE resulted in a small change in grain size; the 0GBE specimen had a grain size of 4.8 µm while the 4GBE specimen had a grain size of

18.8 µm. The CP specimen also exhibited an increase in special fraction and grain size to 0.61 and 13.9 µm, respectively. Table 1 summarizes the results of the different processing methods. An analysis of the error associated with EBSD data was performed for five randomly selected areas, each 1 mm$^2$, from a single specimen. For uniform microstructures, the error in special boundary fraction is ±0.02 and in grain size is ±0.8 µm. It is important to note that the 2GBE, 4GBE and CP specimens had very similar grain sizes after processing and nearly identical special fractions. Although the grain size and special fraction are close, microstructural differences can be observed by examining crystallographic texture. Figure 2 shows orientation maps after processing where the colors correspond to unique crystallographic orientations. The 2GBE and 4GBE specimens have a nearly random texture while the CP specimen shows a strong (001)<100> rolling texture.

Finally, the general boundary cluster size distribution (Figure 3) was determined for each specimen after processing from equivalently-sized areas where the cluster size is normalized to the mean linear intercept [10]. The cluster size distribution for the 0GBE material differs considerably from those of the 2GBE, 4GBE and CP specimens; specifically, much larger general boundary clusters are observed before thermomechanical processing. Although differences are observed between the 2GBE, 4GBE and CP specimens, each of these has its maximum cluster size near 100$\overline{\text{L}}$. The differences in the general boundary connectivity in CP vs. GBE materials are not as drastic as in, e.g., [10].

The results of the GBE processing can be compared to those in [11], from which the GBE parameters were adapted. Most notably, the CP route in that work increased $p$ from 0.15 to 0.57, while four cycles of GBE yielded $p$ = 0.78 [11]. In the present work, the difference in $p$ was less significant and, as will be shown later, cannot be used to explain differences in the properties of the CP and GBE materials. The difference between the effectiveness of GBE here and in [11] likely results from differences in starting materials (e.g., initial grain size and special fraction). In addition, their study used high-purity oxygen-free electrolytic Cu (99.99% pure), while in our study the Cu was 99.9% pure [11]. The purity may have influenced effectiveness of GBE [5], as impurity atoms can minimize the relative energy difference between general and special boundaries due to solute segregation along the boundaries [15]. It is also difficult to compare to the as-processed microstructures in [11] because the crystallographic textures were not reported. Finally, although the authors suggest that the general boundary connectivity varies between GBE and CP materials, no quantitative data were included.

After processing Cu through different routes, the evolution of the GBCD, grain size, and texture was evaluated as a function of annealing time at 700, 800, and 900°C. Table 1 summarizes the grain size and special fraction for each annealed specimen. For specimens without AGG, the standard deviation in the grain size distribution was near the average grain size; AGG specimens typically had standard deviations at least twice the average grain size, indicative of a bimodal distribution. In addition, when AGG was absent, the largest grain was typically <10$\overline{\text{L}}$ while this increased to >10$\overline{\text{L}}$ during AGG. After aging at 700°C, the 4GBE specimens exhibited the greatest microstructural stability in terms of the grain size. The CP specimen, whose grain size and $p$ were initially similar to 4GBE, experienced unpredictable grain growth (e.g., the specimen aged 12 h showed AGG). The microstructural evolution was also characterized by $p$, which increased only slightly in the thermomechanically-processed specimens aged at 700°C (Table 1). The slight increase in $p$ during grain growth is in line with both Ref. [14] and the simulation work of Ono [16], where an increased special fraction during grain growth was found. However, the increase may be insignificant enough that the results can be compared to those of Ref. [17] where no change in GBCD is observed during grain growth.

During annealing at 800°C, both the 2GBE and CP specimens experienced AGG; at 900°C, all specimens except the 4GBE underwent AGG. In the most extreme case (8 hours at 900°C, ~0.86 $T_M$), considerable grain growth was observed in the 4GBE specimen, but the grain size distribution remained relatively stable. The stability of the 4GBE specimen and AGG in the CP specimen are in agreement with Schwartz *et al.* who investigated the effects of aging on GBE copper for up to 16 h at 500 and 700°C [11]. In their study, the 4GBE specimen experienced minimal grain growth, while the specimen analogous to CP experienced abnormal grain growth [11]. The special fraction differed significantly between their GBE and CP specimens and the authors suggested that differences in general boundary connectivity may lead to the observed AGG. However, in the present work, the special boundary fraction in the 2GBE, 4GBE and CP materials is very similar. In addition, within the resolution of the technique, the general boundary connectivity also varies minimally. Therefore, neither of these microstructural descriptors can be reasonably identified as leading to AGG as suggested in [11].

One possible explanation for the microstructural stability of the 4GBE specimen as compared to the CP may be the difference in crystallographic texture of the two specimens which has been shown to affect microstructural evolution [18-20]. This suggests that the AGG observed in our study may be caused by the strong initial texture in the CP specimen. Therefore, further investigation of the AGG specimens was conducted to determine whether the abnormal grains exhibited a preferred crystallographic orientation which could have arisen from the initial texture in the CP material. Figure 4 shows orientation maps of the entire cross-sectional areas of three CP specimens that showed significant AGG and one 4GBE specimen that resisted AGG. The CP specimen annealed 12 h at 700°C showed a moderate amount of abnormal grain growth with areas of stable grain growth. The abnormal grains were oriented with either the <100> or <111> direction parallel to the surface normal. Abnormal grain growth was dominant in the CP specimens that were aged for 6 h at 800°C and 8 h for 900°C; the grains that grew abnormally showed no preferred orientation which suggests that AGG is not driven purely by a texture mechanism. As Figure 4 illustrates, the 4GBE specimen that was aged for 8 h at 900°C showed normal grain growth while maintaining a relatively stable distribution of grain sizes and a random texture.

Furthermore, inspection of the initial microstructures reveals that texture may not be the only cause of AGG. When comparing only the 4GBE and CP specimens, this explanation holds; however, the fact that the 0GBE and 2GBE specimens experienced abnormal grain growth negates initial texture as the only driving force since both specimens exhibited an initially random texture. The 2GBE specimen experienced abnormal grain growth when aged for 18 hours at 800°C and for 8 hours at 900°C while the 4GBE did not. By most microstructural measures (texture, grain size, and special boundary fraction), the two specimens (2GBE and 4GBE) were very similar. In general, AGG results from the extremely high mobility of a subset of grain boundaries which may arise due to a particular crystallographic texture. However, since AGG occurs even in specimens without sharp crystallographic textures, the bulk texture cannot solely drive the onset of AGG. It is possible that the randomly texture samples that underwent AGG had local textures conditions that led to locally high boundary mobility.

## CONCLUSIONS

A study of microstructural stability in commercially-pure copper was presented with the goal of better understanding how microstructure evolves over time at elevated temperatures. The work presented here builds upon the growing body of work concerning GBE and microstructural evolution. The following are the main conclusions:

- GBE processing of commercially-pure copper increased the special boundary fraction from 0.35 to 0.64 while maintaining a random texture. A conventional processing route was also used which resulted in 61% special boundaries and a strong (100)<001> cube texture.
- During annealing, the 4GBE specimen exhibited the greatest microstructural stability, which was attributed to the high special fraction and random texture of the specimen.
- The 2GBE, 4GBE, and CP specimens had similar special boundary fractions and general boundary connectivity; however, the 2GBE and CP specimens undergo AGG which indicates that a more subtle microstructural characteristic, or combination thereof, leads to AGG.

# ACKNOWLEDGEMENTS

# REFERENCES

[1]     Alexandreanu B, Capell B, Was GS. Mater. Sci. Eng. 2001;A300:94.

[2]     Pan Y, Adams BL, Olson T, Panayotou N. Acta Mater. 1996;44:4685.

[3]     Aust KT, Erb U, Palumbo G. Mater. Sci. Eng. 1994;A176:329.

[4]     Palumbo G, King PJ, Aust KT, Erb U, Lichtenberger PC. Scripta Metall. Mater. 1991;25:1775.

[5]     Lin P, Palumbo G, Erb U, Aust KT. Scripta Metall. Mater. 1995;33:1387.

[6]     Shimada M, Kokawa H, Wang ZJ, Sato YS, Karibe I. Acta Mater. 2002;50:2331.

[7]     Lehockey EM, Palumbo G. Mater. Sci. Eng. 1997;A237:168.

[8]     Watanabe T. Res Mechanica 1984;11:47.

[9]     Schuh CA, Kumar M. J. Mater. Sci. 2005;40:847.

[10]    Schuh CA, Kumar M, King WE. Acta Mater. 2003;51:687.

[11]    Schwartz AJ, King WE, Kumar M. Scripta Materialia 2006;54:963.

[12]    Tan L, Sridharan K, Allen TR, Nanstad RK, McClintock DA. J. Nucl. Mater. 2008;374:270.

[13]    Lee SL, Richards NL. Mater. Sci. Eng. 2005;405:74.

[14]    Palumbo G, Aust KT, Proceedings of the Third International Conference on Grain Growth. 1998,vol. 311.

[15]    Palumbo G, Aust KT. Can. Metall. Q. 1995;34:165.

[16]    Ono N, Kimura K, Watanabe T. Acta Mater. 1999;47:1007.

[17]    Hassold GN, Holm EA, Miodownik MA. Mat. Sci. Technol. 2003;19:683.

[18]    Sonnweber-Ribic P, Gruber P, Dehm G, Arzt E. Acta Mater. 2006;54:3863.

[19]    Greiser J, Mullner P, Arzt E. Acta Mater. 2001;49:1041.

[20]    Mishin OV, Gottstein G. Mater. Sci. Eng. 1998;A249:71.

Table 1: Grain size and special boundary fraction after annealing.

Specimens marked AGG underwent abnormal grain growth.

| Temp (°C) | Time (h) | 0GBE | 2GBE | 4GBE | CP |
|---|---|---|---|---|---|
| | | Grain size (µm) | | | |
| RT | 0 | 4.8 | 14.0 | 18.8 | 13.9 |
| 700 | 2 | 15.0 | 17.5 | 17.9 | AGG |
| | 12 | 14.3 | 17.3 | 16.1 | AGG |
| | 36 | 13.1 | AGG | 17.3 | 14.5 |
| | 108 | 15.1 | 16.8 | 19.8 | 15.8 |
| 800 | 6 | 14.9 | 14.7 | 20.1 | AGG |
| | 18 | 15.5 | AGG | 20.1 | AGG |
| 900 | 8 | AGG | AGG | 44.1 | AGG |
| | | Special boundary length fraction | | | |
| RT | 0 | 0.35 | 0.62 | 0.64 | 0.61 |
| 700 | 2 | 0.54 | 0.60 | 0.68 | AGG |
| | 12 | 0.57 | 0.66 | 0.70 | AGG |
| | 36 | 0.65 | AGG | 0.69 | 0.65 |
| | 108 | 0.64 | 0.64 | 0.70 | 0.65 |
| 800 | 6 | 0.66 | 0.71 | 0.71 | AGG |
| | 18 | 0.68 | AGG | 0.70 | AGG |
| 900 | 8 | AGG | AGG | 0.74 | AGG |
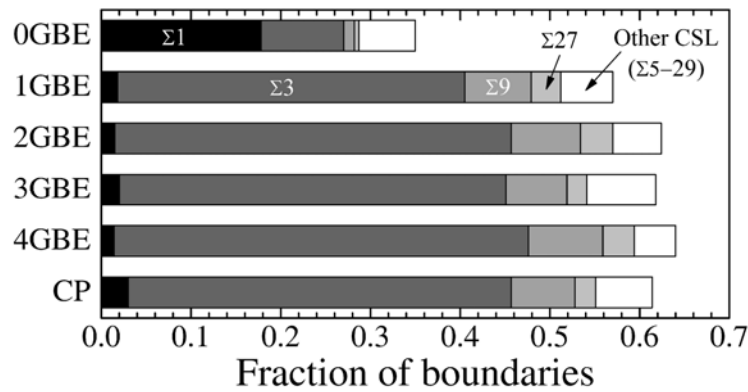


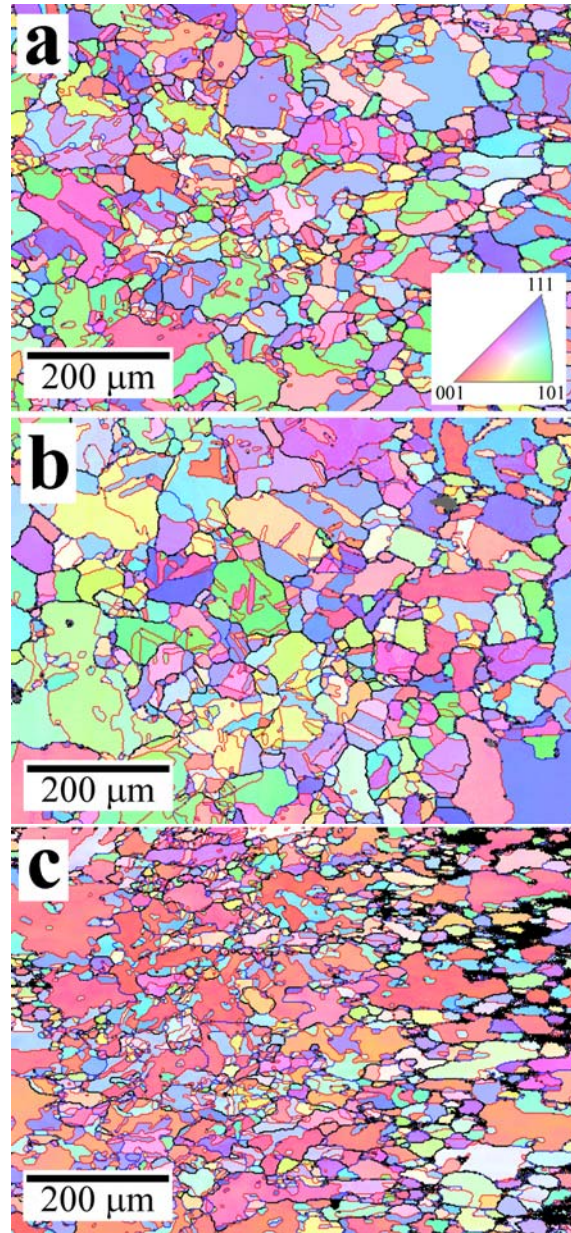Figure 1: Grain boundary character distribution of as-processed specimens prior to annealing.

Figure 2: Orientation map for (a) 2GBE, (b) 4GBE, and (c) CP specimens after processing; grain colors correspond to unique crystallographic orientations as given in the inset legend. Black lines correspond to general grain boundaries, red lines to Σ3 boundaries, and blue lines to other CSL (Σ ≤ 29) boundaries.
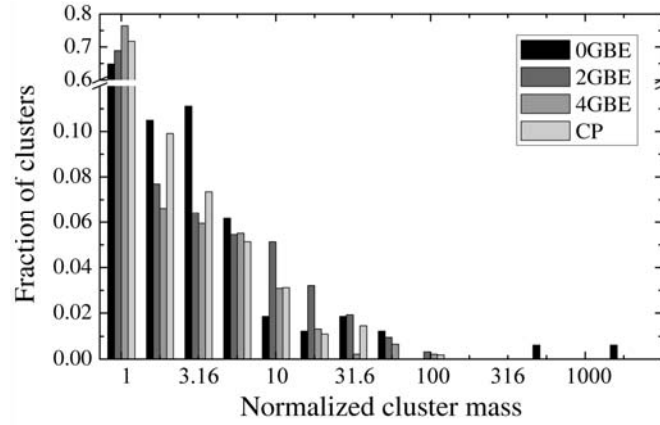
Figure 3: Cluster size distribution from an area $1225\overline{L}^2$ for as-processed specimens. Cluster mass is given in multiples of the mean linear intercept grain size.
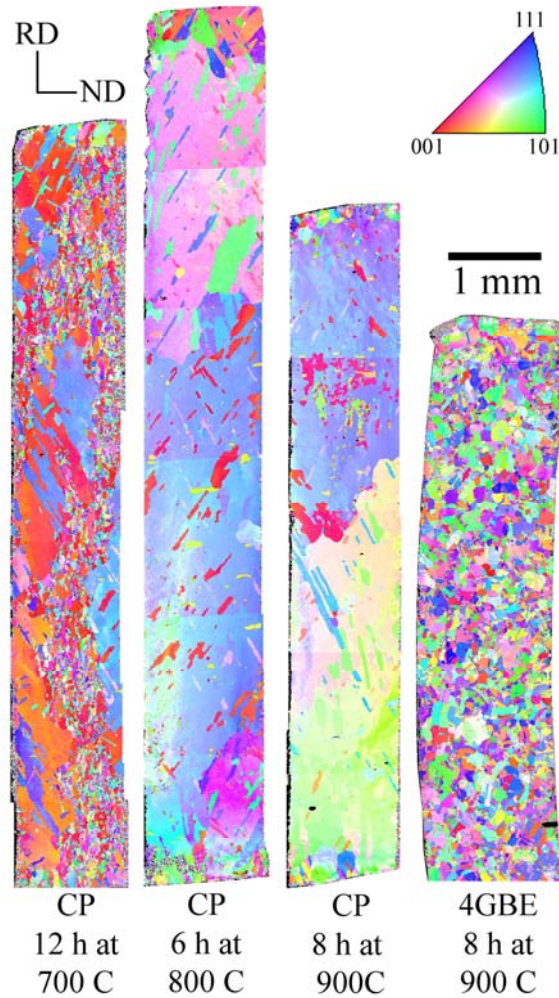


Figure 4: Orientation maps for CP and GBE specimens after annealing which illustrate the extent of abnormal grain growth in the CP specimens and its absence in the 4GBE specimen.